Extended Abstracts of the 2006 International Conference on Solid State Devices and Materials, Yokohama, 2006, pp. 58-59

C-1-4

Equivalent Circuit Model for On-Chip Variable Inductor

Tackya Yammouch, Koichi Ishida, Kenichi Okada and Kazuya Masu
Integrated Research Institute, Tokyo Institute of Technology,
4259-R2-17 Nagatsuta, Midori-ku, Yokohama 226-8503, Japan.
Tel. : +81-45-924-5031 Fax. : +81-45-924-5166 E-mail : paper@lsi.pi.titech.ac.jp

I. Introduction

Recently, demand for wide-band RF circuits has been increasing for ubiquitous computing era. Variable passive components such as variable capacitors and variable inductors are quite useful for realizing the wide-band RF circuits. Several variable inductors using MEMS [1]–[6] have been proposed. However, the lack of an accurate model for the variable inductors makes design of the wide-band RF circuits challenging. Thus, in this work, we propose an equivalent circuit model for the variable inductors, and evaluate the model with measurement results.

II. Equivalent Circuit Model

Figure 1 shows the schematic of the on-chip variable inductor. The inductor consists of a wiring line and a metal plate above. Figure 2 shows the cross section of the inductor. Magnetic flux induced by the wiring penetrates the metal plate, and eddy current is generated shch as a white ring of arrow in Fig. 2. Because the eddy current also generates counteractive magnetic flux canceling the original flux, inductance decreases. The inductance varies according to the height of metal plate. MEMS actuator [7] are used for vertical movement of the metal plate.

Figure 3 shows a conventional single-pi equivalent circuit [8] for on-chip inductors. Figure 4 shows the proposed model that has metal plate and substrate networks to characterize the variation of inductance and quality factor. L_1 and R_1 are inductance and resistance of wiring line, respectively. L_2 and R_2 are equivalent inductance and resistance of metal plate, $k_{12}\,(= M_{12}/\sqrt{L_1 L_2})$ is an equivalent coupling coefficient between the wiring line and the metal plate. L_3 and R_3 are equivalent inductance and resistance of silicon substrate, respectively. k_{13} and k_{23} are an equivalent copling coefficient between spiral metal and silicon substrate and one between metal plate and silicon substrate, respectively. $C_{\rm ox}$ is capacitance between the wiring and the substrate, and $C_{\rm Si}$ is substrate capacitance. $R_{\rm Si}$ is substrate resistance.

In this model, k_{12} and k_{23} are functions of the height of metal plate h. The other parameters are independent to h.

III. Model Verification

To evaluate the accuracy of the proposed model, a spiral inductor shown in Fig. 5 was fabricated using $0.18\,\mu$m five-metal CMOS technology. The inductor has 3 turns, an outer diameter D of $400\,\mu$m, line width w of $20\,\mu$m and line spacing s of $1.2\,\mu$m. Two-port S-parameters were measured using an Agilent 8720ES network analyzer and RF probes. To characterize the intrinsic inductor, the pad parastics were de-embeded with the measurement of open and short pads. The metal plate was manually moved using a micro manipulater.

The impedance Z of the equivalent circuit shown in Fig. 4 is calculated as follows:

$$Z = f\Big(\omega, L_1, R_1, \frac{R_2}{L_2}, \frac{R_3}{L_3}, C_{\rm ox}, C_{\rm Si}, R_{\rm Si}, k_{12}(h), k_{13}, k_{23}(h)\Big). \qquad (1)$$

R_2/L_2 can be neglected over 100 MHz. Their frequency independent parameters were extracted by fitting the proposed model to the measured Y-parameters using ADS optimization routines. Table I shows the extracted parameters.

To evaluate the model validity, the equivalent series inductance L and the quality factor Q were calculated. Figure 6(a) shows the measured and modeled L. Figure 6(b) shows the Q curves. As can be seen from the figures, the L and Q of the proposed model agree with the measured data with L error of ± 0.3 nH and Q error of 0.2.

Figure 7 shows extracted k values as a function of h. $k_{12}(h)$ and $k_{23}(h)$ can be approximated with exponential functions shown in Fig. 7.

IV. Conclusions

We have proposed a novel equivalent circuit model for variable inductors. The proposed model consists of a conventional single-pi circuit, a network for the metal plate, one for silicon substrate, and coupling coefficients among their networks. The evaluation using measurement has demonstrated the validity of the proposed model. The proposed model can be easily implemented in SPICE-compatible simulators to design wide-band RF circuits.

References

[1] Y. Yoshihara, H. Sugawara, H. Ito, K. Okada, and K. Masu: IEICE Trans. on Fundamentals of Electronics, Communications and Computer Sciences **E-88A** (2005) No. 2, 507.
[2] Y. Yokoyama, T. Fukushige, S. Hata, K. Masu, and A. Shimokohbe: Jpn. J. Appl. Phys. **42** (2003) 2190.
[3] S. Gomi, Y. Yokoyama, H. Sugawara, H. Ito, K. Okada, H. Hoshino, H. Onodera, and K. Masu: *Proc. Int. Conf. on Solid State Devices and Materials* (2003) p. 398.
[4] H. Sugawara, Y. Yokoyama, S. Gomi, H. Ito, K. Okada, H. Hoshino, H. Onodera, and K. Masu: Jpn. J. Appl. Phys. **43** (2004) 2293.
[5] H. Sugawara, H. Ito, K. Okada, K. Itoi, M. Sato, H. Abe, and K. Masu: *Proc. Top. Meet. on Silicon Monolithic Integrated Circuits in RF Systems* (2004) p. 187.
[6] H. Sugawara, Y. Yoshihara, H. Ito, K. Okada, and K. Masu: *Proc. 34th European Microwave Conference* (2004) p. 701.

[7] V. M. Lubecke and J. C. Chiao: *Proc. IEEE 4th Int. Conf. on Telecommunications in Modern Satellite, Cable and Broadcasting Services* (1999) p. 382.

[8] C. P. Yue and S. S. Wong: IEEE Trans. on Electron Devices, **47** (2000) No. 3, 560.

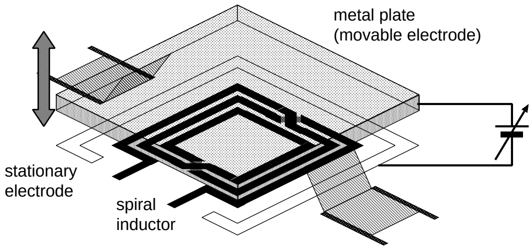

Fig. 1. Structure of variable inductor.

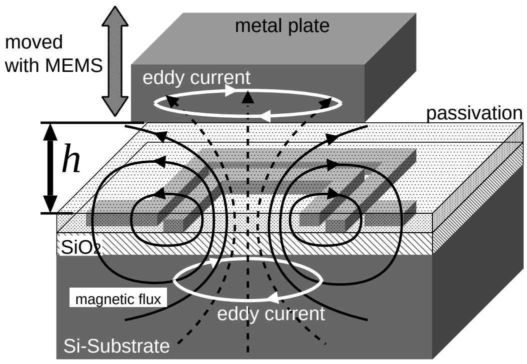

Fig. 2. Cross section of the variable inductor.

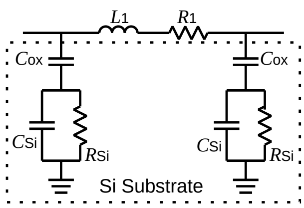

Fig. 3. Conventional single-pi model.

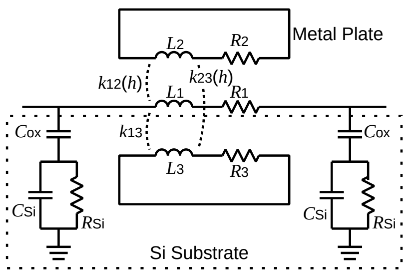

Fig. 4. Proposed model for variable inductors.

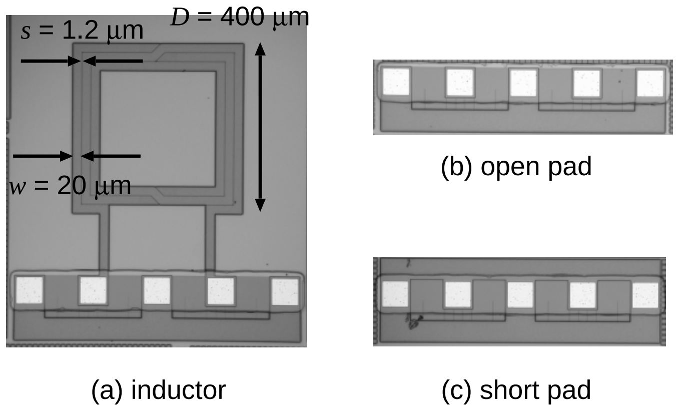

Fig. 5. Micrographs of DUT: (a) the on-chip inductor, for de-embedding (b) open pad, and (c) short pad.

TABLE I

EXTRACTED MODEL PARAMETERS FOR THE INDUCTOR.

param	value	param	value
L_1	5.6 nH	$C_{\rm ox}$	0.33 pF
R_1	8.5 Ω	$C_{\rm Si}$	0.11pF
R_3/L_3	12.7 GHz	$R_{\rm Si}$	17 Ω
k_{13}	0.49		
$k_{12}(h = 15[\mu m])$	0.26	$k_{23}(h = 15[\mu m])$	0.22
$k_{12}(h = 35[\mu m])$	0.53	$k_{23}(h = 35[\mu m])$	0.37
$k_{12}(h = 105[\mu m])$	0.67	$k_{23}(h = 105[\mu m])$	0.39

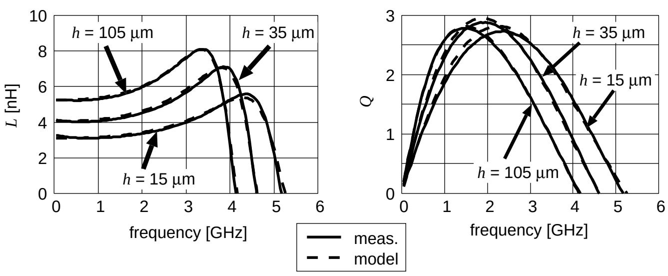

Fig. 6. Measured and modeled value of L and Q.

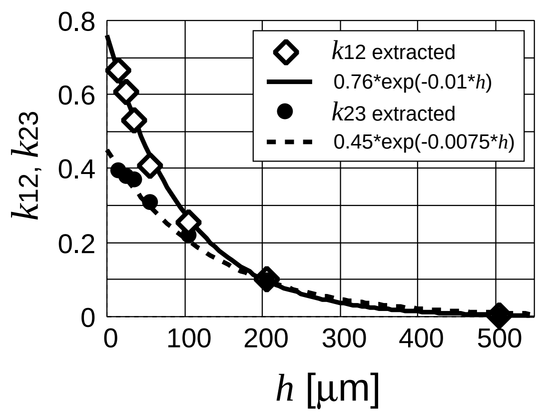

Fig. 7. Extracted k values and fitting functions that approximate k.